Princeton Plasma Physics Laboratory

PPPL- 4944

PPPL- 4944

Plasma Mass Filtering for Actinides/ Lanthanides Separation

R. Gueroult and N.J. Fisch

October 2013

Prepared for the U.S. Department of Energy under Contract DE-AC02-09CH11466.

Princeton Plasma Physics Laboratory
Report Disclaimers

Full Legal Disclaimer

This report was prepared as an account of work sponsored by an agency of the United States Government. Neither the United States Government nor any agency thereof, nor any of their employees, nor any of their contractors, subcontractors or their employees, makes any warranty, express or implied, or assumes any legal liability or responsibility for the accuracy, completeness, or any third party's use or the results of such use of any information, apparatus, product, or process disclosed, or represents that its use would not infringe privately owned rights. Reference herein to any specific commercial product, process, or service by trade name, trademark, manufacturer, or otherwise, does not necessarily constitute or imply its endorsement, recommendation, or favoring by the United States Government or any agency thereof or its contractors or subcontractors. The views and opinions of authors expressed herein do not necessarily state or reflect those of the United States Government or any agency thereof.

Trademark Disclaimer

Reference herein to any specific commercial product, process, or service by trade name, trademark, manufacturer, or otherwise, does not necessarily constitute or imply its endorsement, recommendation, or favoring by the United States Government or any agency thereof or its contractors or subcontractors.

PPPL Report Availability

Princeton Plasma Physics Laboratory:

http://www.pppl.gov/techreports.cfm

Office of Scientific and Technical Information (OSTI):

http://www.osti.gov/bridge

Related Links:

U.S. Department of Energy

Office of Scientific and Technical Information

Fusion Links

Plasma mass filtering for actinides/lanthanides separation

R Gueroult, N J Fisch

Princeton Plasma Physics Laboratory, Princeton University, Princeton, NJ 08543 USA

E-mail: rgueroul@pppl.gov

Abstract. Separating lanthanides from actinides is a key process in reprocessing nuclear spent fuel. Plasma mass filters, which operate on dissociated elements, offer conceptual advantages for such a task as compared to conventional chemical methods. The capabilities of a specific plasma mass filter concept, called the Magnetic Centrifugal Mass Filter (MCMF), are analyzed within this particular context. Numerical simulations indicate separation of Americium ions from a mixture of lanthanides ions for plasma densities of the order of 10^{12} cm^{-3}, and ion temperatures of about 10 eV. Separating small fractions of heavy elements from a larger volume of lighter ones is shown to enhance the separation capabilities.

1. Introduction

The interest of plasmas to discriminate elements based on their mass has long been recognized, and can be traced as far back as the Calutron device [1] during the Manhattan project. The potential of rotating plasma configurations was quickly identified [2]. These configurations present the advantage, as compared to their classic gaseous or liquid counterparts, to operate at larger rotation speeds, offering in principle larger processing rate.

The vast majority of the research conducted in this field has been dedicated to isotope separation [3, 4, 5], for which the mass difference of the elements to be separated is small. This small mass difference in turn usually limits the achievable throughput. More recently, plasma mass filtering has been considered for nuclear waste remediation [6]. In this case, the mass difference can be significant, allowing theoretically much larger throughputs. Two different configurations relying on different mass discrimination schemes have been proposed to fulfill this objective. In the Ohkawa filter [7], mass separation is achieved as a result of the existence of a charge to mass threshold for ion confinement. Unconfined heavy ions are therefore collected radially, while light elements exit axially. On the other hand, in the Magnetic Centrifugal Mass Filter (MCMF) [8, 9], ions of different masses are collected at different axial end of the device. This is made possible by using an asymmetric collisional rotating plasma.

The fact that plasma mass filters operate irrespectively of the input stream chemical form makes them attractive for separation processes which are simultaneously chemically challenging and of high added value. Among these is the separation of lanthanides from actinides, within the process of nuclear spent fuel reprocessing [10]. Partitioning and transmutation of the long-lived minor actinides into shorter-lived or stable elements is considered as a way to decrease the mandatory storage time of remaining nuclear waste to a few hundreds years, in place of several thousands years [11, 12]. However, a prerequisite to this step consists in the separation of lanthanides from minor actinides because of the large lanthanides' neutron capture cross section [13]. From a chemical standpoint, this separation is made particularly difficult by the chemical similarities existing between the two groups of elements [10, 14].

In this paper, the potential of the MCMF is evaluated with respect to separating lanthanides from actinides. First, in Sec. 2, the typical composition of spent nuclear fuel is used to identify a realistic plasma composition for this test study. In Sec. 3, single particle ion trajectory modeling is conducted. These simulations allow estimating realistic plasma parameters for the considered separation process. In Sec. 4, the model is then refined to analyze the influence of a multi-species plasma on the separation properties. In Sec. 5, the main findings are summarized.

2. Plasma composition of interest

Nuclear spent fuel recovered from reactors consists mostly (about 94 % in mass) of unburned uranium fuel. This unaffected fuel can be separated and processed for additional use, through the Purex (Plutonium Uranium Refining by Extraction) process [15]. This process, globally in use around the world in reprocessing plants, allows recovering about 99.9 % of both the Uranium and Plutonium present in the spent fuel stream. As shown in Fig. 1, the remainder of the stream (over 40 different

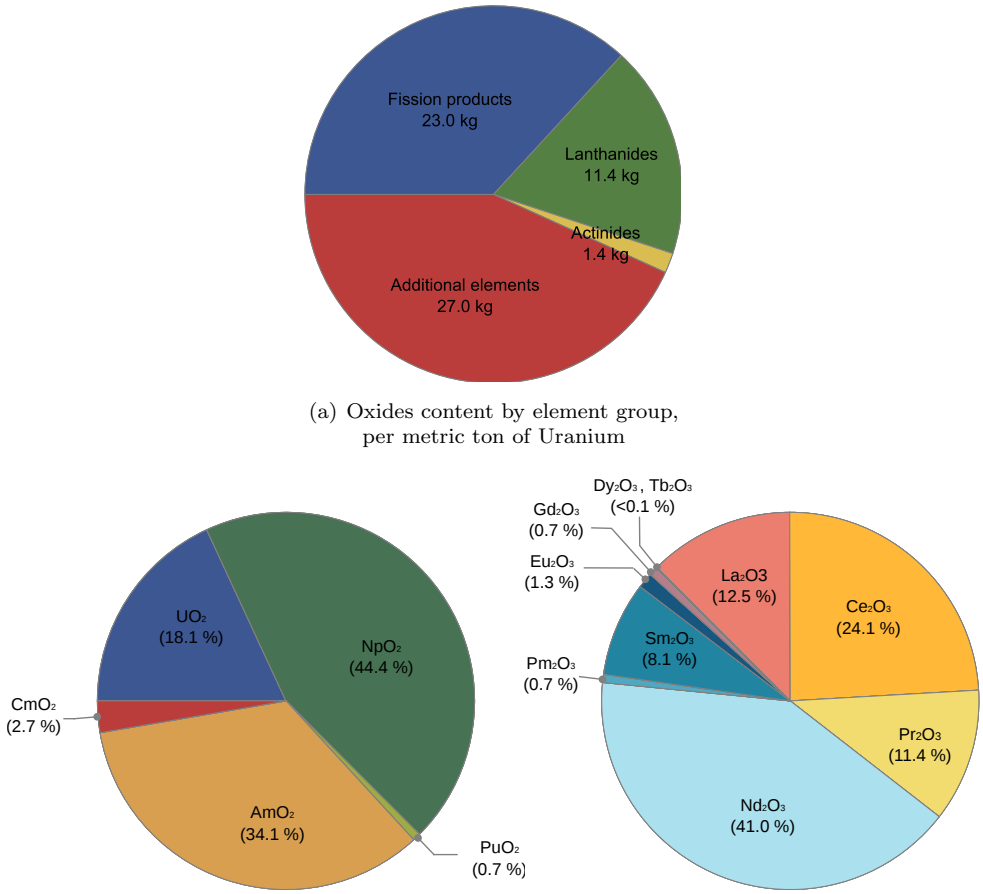

(a) Oxides content by element group, per metric ton of Uranium

(b) Distribution within actinides elements

(c) Distribution within lanthanides elements

Figure 1. Composition of nuclear spent fuel for a standard 33 GW/t reactor, after 3 years cooling, data from [16].

elements) is made of various fission products, lanthanides, minor actinides, as well as additional elements resulting from the PUREX treatment. The current industrial approach consists in stocking this stream for a year before vitrification and permanent geological repository.

At this stage, the large majority of the long-term radioactivity hazard originates from the minor actinides and daughter elements. Looking at Fig. 1(b), one can see that, apart from the non-recovered Uranium and Plutonium, the hazard lies in the presence of Neptunium, Americium and Curium. Transmutation of these elements into shorter-lived elements is one of the options for decreasing the spent fuel long-term biological hazard. However, because of the large neutron capture cross-section exhibited by lanthanides [13], actinides have to be separated from lanthanides *a priori*. An upgrade of the chemical PUREX process, called the advance PUREX, has been developed to recover Neptunium in addition to Uranium and Plutonium [17]. On the other hand, the chemical separation of Americium and Curium from the lanthanides is made particularly difficult because of the chemical similarities existing between these

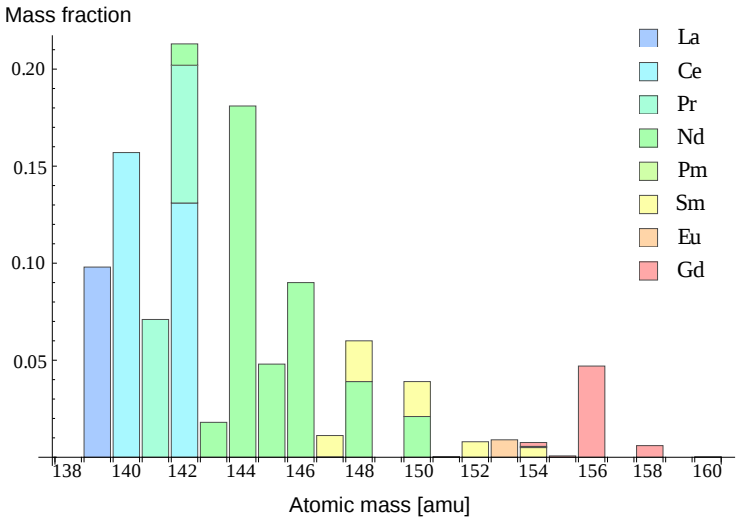

Figure 2. Isotopic distribution of mass within the lanthanides fission products, from [18]. The average mass is 144 amu.

elements [10, 14]. Note that among these two elements, only the removal of Americium is strictly required. As a matter of fact, the two main Curium isotopes (^{243}Cm and ^{244}Cm) decay into Plutonium (^{239}Pu and ^{240}Pu), with half-lives of respectively 29 and 18 years. Curium could therefore be stored and monitored with the lanthanides, until the naturally formed Plutonium can be recovered. On the other hand, ^{241}Am, which is the main Americium isotope, decays into Neptunium with a half-life of about 432 years, making its *a priori* removal a requirement.

In light of these facts, the most challenging process appears to lie in the separation of Americium, and more specifically ^{241}Am, from a mixture of lanthanides. To assess the potential of a plasma mass filter for this task, one can assume a characteristic plasma composition on the basis of the lanthanide group elements distribution such as depicted Fig. 1(c). More precisely, the isotopic mass distribution within the lanthanides group [18], as plotted in Fig. 2, indicates an average mass of 144 amu. The idealized case considered in the remaining of this paper is consequently the separation of ^{241}Am ions from 144 amu ions. Based on the relative oxides masses, the corresponding plasma composition would be about 0.04 Americium ion for one 144 amu ion.

3. Evaluation of the plasma filter performance

3.1. Numerical simulation model

The particular plasma mass filter considered here is the so called Magnetic Centrifugal Mass Filter (MCMF) [8]. As illustrated in Fig. 3, mass separation in this device relies on asymmetric confinement properties at each end of the device. Confinement at one end is dominated by centrifugal forces, and thus mass dependent. At the other end, confinement is dominated by magnetic forces, which are mass independent. The requirements of mass discrimination with respect to plasma parameters have been

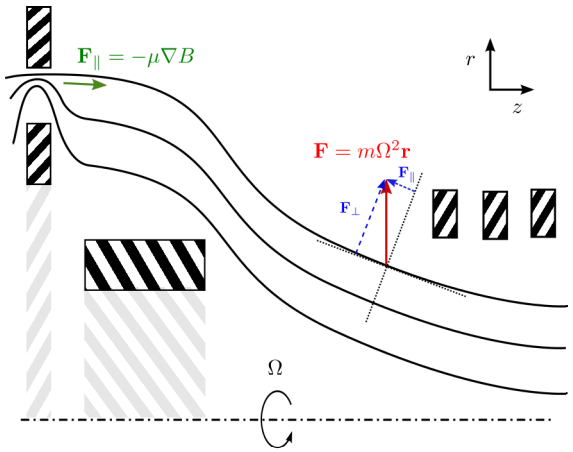

Figure 3. Cut view of the MCMF magnetic field topology ($r - z$ plane). Solid lines represent the magnetic field lines; the dashed-dotted line indicates the axis of symmetry; hatched boxes represent magnetic coils.

previously discussed [9].

In light of the potential interest of a plasma mass filter for separating actinides from lanthanides introduced in Sec. 2, the capabilities of the MCMF for this particular purpose are studied by means of numerical simulations. The physics of the model is described elsewhere [9]. Here, we only give a brief summary of the numerical model. It consists in a 3-d modeling of individual ion trajectories within the rotating collisional plasma. Ion motion is calculated from the Lorentz force resulting from the externally prescribed electric and magnetic fields, as well as from Coulomb collisions computed in the rotating frame. The simulation is run until the particle exits through one of the axial ends of the device, or, alternatively, is lost radially. Separation properties are estimated by computing statistics over a large number of ion trajectories.

3.2. Achievable plasma parameters and typical separation

The device dimensions considered here are identical to the ones previously used [9], namely 50 cm in radius and 60 cm in length. However, the magnetic and electric field strength and topology differ slightly. The magnetic field map is plotted in Figure 4. As compared to [9], the magnetic field topology has been modified to maximize the radial extent of the confinement at the mirror throat (heavy element extraction side). The electric field, set by specifying a given electric potential to individual magnetic field line, dictates the rotation speed through the $\mathbf{E} \times \mathbf{B}$ drift.

A first step towards assessing the MCMF separation capabilities consists in simulating the behavior of one specific ion with its parent specie. The results obtained for an ion of 144 amu as well as for a ^{241}Am ion are given in Fig. 5. The results globally display a relatively large spectrum of separation values while maintaining the radial losses under 15%. As an example, for a density of 10^{12} cm^{-3} and a plasma rotation speed $v_{\mathbf{E}\times\mathbf{B}}$ at the ion injection point of about 4.25 km.s^{-1} (data points in grey in Figure 5), about three ^{241}Am ions are collected on the heavy side for one collected on the light side. For the same parameters, this ratio is about 1.33 for the 144 amu test

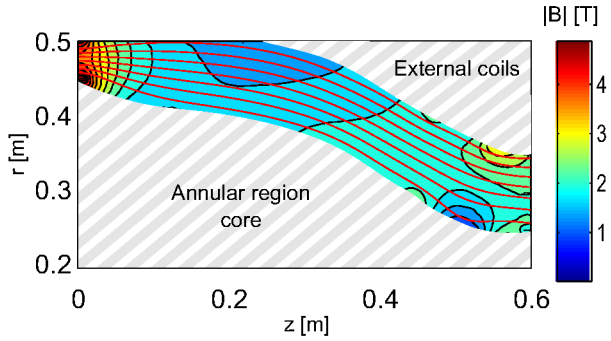

Figure 4. Magnetic field map used for the simulations. Red lines represent the magnetic field lines; hatched regions depict respectively the inner core region, used to bend the magnetic field lines, and the outer region, where the magnetic coils producing the magnetic field are positioned. The region of interest is therefore annular.

ion. Looking at the rotation speed dependence, one can see that an increase of the rotation speed enhances the mass dependence of the properties, which is depicted by an increase of the distance between same color data points. This trend is combined with a decrease of the collection at the light side, in favor of the heavy side, as a result of the larger centrifugal potential barrier to be overcome at the light side end. This translates into a shift of the data points to the left in Fig 5. Moving now to the influence of the plasma density, an increase of n leads to a combined increase of the collection on the light side (shift to the right) and of the radial losses (shift upward). The light side collection increase can be explained by the higher collisionality, which enhances the ion-ion pitch angle scattering allowing ion extraction on the light side [9]. The higher collisionality explains as well the radial losses increase, since the ion motion perpendicular to the magnetic field lines results from collisional diffusion.

These preliminary simulation results indicate that the MCMF is suitable to operate on lanthanides and Americium, for plasma densities up to a few 10^{12} cm^{-3}. However, these results have been obtained by simulating the interaction of a single ion with its sole parent specie. Since the MCMF separation scheme relies on ion-ion collisions, it stands to reason that a modification of the plasma composition would affect the separation properties of this device. In addition, as discussed in Sec. 2, the plasma composition expected for the particular Americium-lanthanides separation process is asymmetric, with lanthanides making most of the stream, so that this dependence requires a more careful examination.

4. Influence of the plasma composition

The influence of plasma composition on the separation capabilities is investigated by modifying the previous numerical model. The trajectory of a single ion (144 amu or ^{241}Am) is now computed by considering its interaction with a plasma made of both ion species. The total plasma density is $n = n^{(144)} + n^{(241)}$, where $n^{(144)}$ and $n^{(241)}$ denote respectively the light (144 amu) and heavy (^{241}Am) ion densities. The plasma composition ratio $\eta = n^{(144)}/[n^{(144)} + n^{(241)}]$ is introduced in order to investigate the sensitivity of the plasma separation properties as a function of the plasma composition.

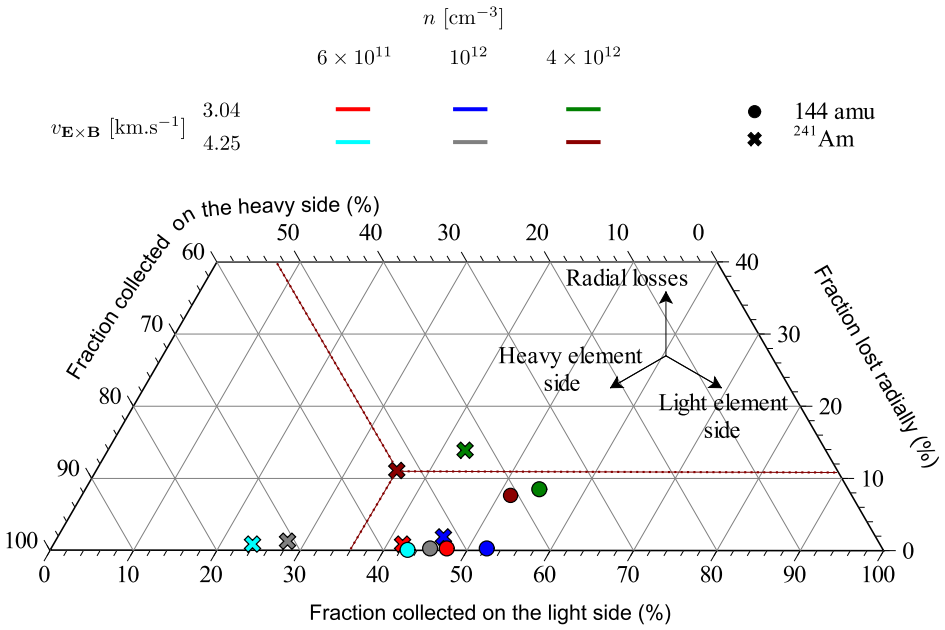

Figure 5. Separation properties obtained for various plasma densities and rotation speeds. In this figure, the fraction collected on the light side increases from left to right, the fraction collected on the heavy side increases from right to left, and the fraction lost radially increases from bottom to top. As an example, the dark-red cross (^{241}Am, 4×10^{12} cm^{-3}, 4.25 km.s^{-1}) reads 36% collected on the light side, 53% collected on the heavy side, and 11% lost radially.

Typical results obtained for constant plasma number density (similar to the ones highlighted in Fig. 5), but varying plasma compositions, are presented in Fig. 6. Looking at the ^{241}Am data, it can be seen that a decrease of η, that is to say a decrease of the heavy ions fraction in favor of the lighter ions, leads to an increase of the collection on the heavy side, and a corresponding decrease of the collection on the light side. The separation factor, computed as the ratio of heavy to light streams fraction, varies here from 1.64 for $\eta = 1$ to 1.78 for $\eta = 0$. A plausible explanation for this evolution is the weaker pitch-angle scattering experienced by heavy ions on light ones, as compared to heavy-heavy ion collisions. However, the consideration of pitch angle scattering is not sufficient explanation by itself, as demonstrated by the evolution of the data corresponding to light ions (144 amu) in Fig. 6. Indeed, although a similar decrease of pitch angle scattering as η decreases is expected to enhance the collection on the heavy side at the expense of the collection to the light side, an opposite behavior is observed as η decreases under about 0.5 in this particular case.

An explanation for this trend can be proposed by introducing the Langevin friction and diffusion coefficients [19] for a particle α of velocity v interacting with an ion population β of isotropic velocity distribution,

$$\mathcal{F}^{(\alpha)}(v) = -n^{(\beta)}\Gamma_p^{(\alpha\beta)}\frac{8\pi}{v^2}\int_0^v f^{(\beta)}(w)w^2dw \tag{1a}$$

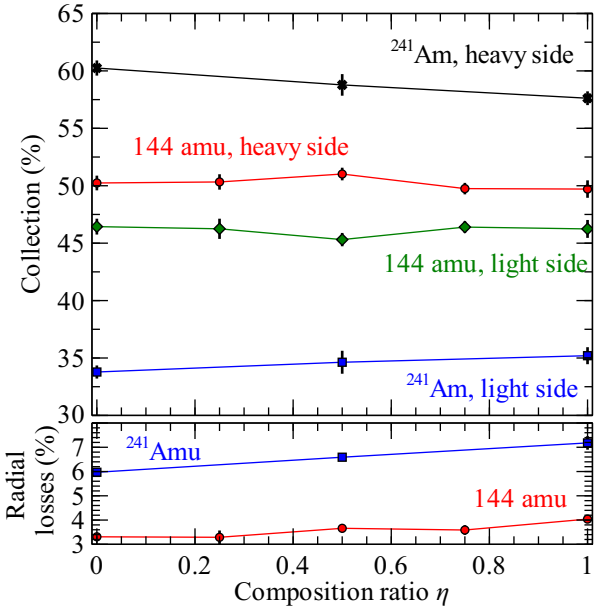

Figure 6. Evolution of the separation properties as a function of the composition ratio $\eta = n^{(144)}/[n^{(144)} + n^{(241)}]$. Plasma parameters: $n = n^{(144)} + n^{(241)} = 10^{12}$ cm^{-3}, $T_i = 10$ eV, plasma rotation speed at injection point $v_{\mathbf{E}\times\mathbf{B}} = E/B \sim 3$ km.s^{-1} $\sim 0.83 {v_{th}}^{(144)}$.

$$\mathcal{D}_{\parallel}^{(\alpha)}(v) = n^{(\beta)}\Gamma_p^{(\alpha\beta)}\frac{8\pi}{3}\left[\frac{1}{v^3}\int_0^v f^{(\beta)}(w)w^4dw + \int_v^\infty f^{(\beta)}(w)wdw\right] \tag{1b}$$

$$\mathcal{D}_{\perp}^{(\alpha)}(v) = n^{(\beta)}\Gamma_p^{(\alpha\beta)}\frac{4\pi}{3}\left[\frac{1}{v^3}\int_0^v f^{(\beta)}(w)w^2(3v^2 - w^2)dw + 2\int_v^\infty f^{(\beta)}(w)wdw\right], \tag{1c}$$

where

$$\Gamma_p^{(\alpha\beta)} = q_\alpha^2 q_\beta^2 [4\pi\epsilon_0^2 m_\alpha^2]^{-1/2} \ln\Lambda, \tag{2}$$

with q the particle charge, m the particle mass, n the number density, $\ln\Lambda$ the Coulomb logarithm and $f(v)$ the velocity distribution function. The corresponding coefficients, obtained for a light ion (144 amu) interacting with a plasma composed of two distinct 10 eV Maxwellian distributions $f^{(\beta)}(v) = [m^{(\beta)}/(2\pi k_B T_i)]^{3/2} \exp[-m^{(\beta)}v^2/(2k_B T_i)]$, where $(\beta) = (144)$ and $(\beta) = (241)$, are plotted in Fig. 7. As mentioned previously, the perpendicular diffusion coefficient $\mathcal{D}_\perp$ increases with η, meaning that lighter ions are less efficient at redirecting ions velocity vector towards the axial ends of the device than heavier ones. This effect can explain, as invoked for ^{241}Am, an increase of the collection on the heavy side at the expense of the light side a η decreases. This collisionality decrease explains as well the lower radial losses levels observed for low η values. However, looking now at the friction coefficient $\mathcal{F}$ in Fig. 7, $\mathcal{F}$ scales as η for low v/v_{th} ratios. This indicates that slowing down decreases as the mean plasma ion mass decreases. Such an effect should limit the collection of ions on the heavy side, since a slower decrease of the ion magnetic moment μ makes it harder for the ions to exit through the magnetic mirror. In addition, better confinement on the heavy side naturally brings a larger ion collection on the light side, as the increased confinement

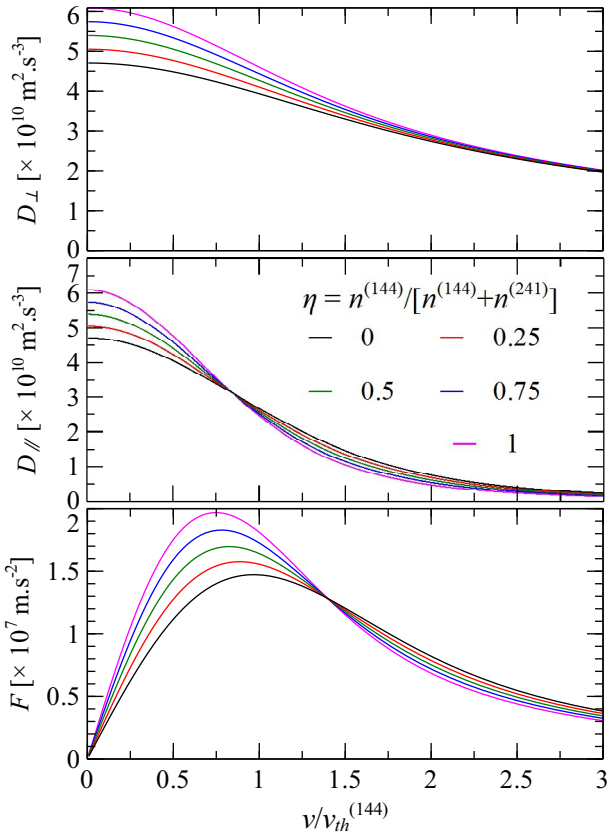

Figure 7. Langevin formalism perpendicular et parallel diffusion coefficients ($\mathcal{D}_\perp$ and $\mathcal{D}_\parallel$), and friction coefficient ($\mathcal{F}$) for various values of the composition ratio $\eta = n^{(144)}/[n^{(144)}+n^{(241)}]$. Light ion ($m_L = 144$ amu) impacting on a mixture of 144 amu and ^{241}Am ions. Plasma parameters: $n = n^{(144)} + n^{(241)} = 10^{12}$ cm^{-3}, $T_i = 10$ eV isotropic Maxwellian velocity distribution.

time offers better chances for an ion velocity vector to be redirected towards the light collection side. Perpendicular diffusion $\mathcal{D}_\perp$ and friction $\mathcal{F}$ dependences on the plasma composition η consequently yield opposite effects.

A justification for the difference observed between the light and heavy ion separation property, as it evolves with η, might lie in the initial velocity of these ions. Ions are initialized at rest in the lab frame, that is to say with the rotation velocity in the rotating frame. In this frame, both ions have consequently the same initial velocity but different kinetic energies ε as a result of their mass difference. For the $v_{\mathbf{E}\times\mathbf{B}} \sim 3$ km.s^{-1} case analyzed, light and heavy ions have initially kinetic energies $\varepsilon^{(144)} = 6.9$ eV and $\varepsilon^{(241)} = 11.7$ eV. Considering the $T_i = 10$ eV background ion temperature (*i. e.* ${v_{th}}^{(144)} \sim 3.6$ km.s^{-1} and ${v_{th}}^{(241)} \sim 2.8$ km.s^{-1}), heavy ions are initially supra-thermal, while light ions are initially sub-thermal. Looking at Eq. 1a,

one can show that $\partial\mathcal{F}/\partial\eta$ decreases with v for

$$v \geq {v_{th}}^{(144)} \sqrt{\frac{\pi}{2} \frac{\ln\left[m^{(241)}/m^{(144)}\right]}{m^{(241)}/m^{(144)} - 1}} \sim 0.72 \; {v_{th}}^{(144)}. \tag{3}$$

The influence of a plasma mean mass decrease on $\mathcal{F}$ is consequently expected to be larger for smaller v/v_{th} ratios, such as likely to occur for light elements. This could explain the fact that the separation increase with decreasing η is partly mitigated for light ions, but not for heavy ions.

In summary, it appears that the lower the fraction of heavy elements in the input stream, the higher is the separation factor for heavy elements when the background ion temperature is set in between the light and heavy initial rotation energies. A low heavy element fraction is typical of the separation of Americium from lanthanides (*c. f.* Sec. 2). Effects on the light elements separation are observed to be more complex and less distinct. A proposed explanation for this difference is the larger influence of the slowing down dependence on the plasma mass composition of light elements.

5. Summary

The transmutation of long-lived minor actinides, such as considered in the development of closed nuclear fuel cycle, requires separating *a priori* these actinides from a larger volume of non radioactive elements exhibiting orders of magnitude larger neutron capture cross-section. A typical example consists in separating ^{241}Am from a mixture of lanthanides elements. From a chemical standpoint, this task is made especially difficult by the similarities existing between these elements. In contrast, plasma mass filters, which operate by nature irrespectively of the input stream chemical form, offer in principle promising alternatives for these separation processes.

Numerical simulations indicate that a particular mass filter configuration, called the Magnetic Centrifugal Mass Filter, might offer separation factors of up to three in a single pass for the particular case of removing ^{241}Am from lanthanides, and that for plasma number densities of about 10^{12} cm^{-3}. Parameter space probing shows that the separation properties can be tuned on a wide range by varying the rotation speed and/or the plasma number densities, while maintaining radial losses to acceptable levels (< 15 %). In addition, it is expected that increasing the device dimensions would limit the radial losses.

For asymmetric plasma compositions where most of the mass is made of light ions, the heavy species tend to separate better than the light species. This is foreseen as an advantage for the particular case of ^{241}Am-lanthanides separation since the mass of ^{241}Am is evaluated to be about only 4.2% of the input stream. More generally, this property would be particularly interesting for any separation process of which the objective consists mainly in isolating heavy elements, such as nuclear waste remediation.

Acknowledgments

This work was supported by US DOE under contracts DE-FG02-06ER54851 and DE-AC02-09CH11466.

References

[1] Lawrence E O 1958 Calutron system
[2] Lehnert B 1971 *Nuclear Fusion* **11** 485– DOI: 10.1088/0029-5515/11/5/010
[3] Krishnan M, Geva M and Hirshfield J L 1981 *Phys. Rev. Lett.* **46** 36–38 DOI: 10.1103/PhysRevLett.46.36
[4] Grossman M W and Shepp T A 1991 *IEEE Transactions on Plasma Science* **19** 1114–1122 DOI: 10.1109/27.125034
[5] Rax J M, Robiche J and Fisch N J 2007 *Phys. Plasmas* **14** 043102–8 DOI: 10.1063/1.2717882
[6] Freeman R, Agnew S, Anderegg F, Cluggish B, Gilleland J, Isler R, Litvak A, Miller R, O'Neill R, Ohkawa T, Pronko S, Putvinski S, Sevier L, Sibley A, Umstadter K, Wade T and Winslow D 2003 *AIP Conf. Proc.* **694** 403–410 DOI: 10.1063/1.1638067
[7] Ohkawa T and Miller R L 2002 *Phys. Plasmas* **9** 5116–5120 DOI: 10.1063/1.1523930
[8] Fetterman A J and Fisch N J 2011 *Phys. Plasmas* **18** 094503–3 DOI: 10.1063/1.3631793
[9] Gueroult R and Fisch N J 2012 *Phys. Plasmas* **19** 122503–6 DOI: 10.1063/1.4771674
[10] Peterman D R, Greenhalgh M R, Tillotson R D, Klaehn J R, Harrup M K, Luther T A, Law J D and Daniels L M 2008 Separation of minor actinides from lanthanides by dithiophosphinic acid extractants *In Proceedings of the 2008 Internation Solvent Extraction Conference (ISEC)*
[11] Magill J, Berthou V, Haas D, Galy J, Schenkel R, Wiese H W, Heusener G, Tommasi J and G Y 2003 *Nuclear Energy* **42** 263–277
[12] on America's Nuclear Future B R C 2012 *Reactor and Fuel Cycle Technology Subcommittee report to the full commission updated report* (Washington, DC: Blue Ribbon Commission on America's Nuclear Future)
[13] Mathur J N, Murali M S and Nash K L 2001 *Solvent Extraction and Ion Exchange* **19** 357–390 DOI: 10.1081/SEI-100103276
[14] Morss L R, Edelstein N M and Fuger J (eds) 2011 *The Chemistry of the Actinide and Transactinide Elements* (Springer Netherlands) DOI: 10.1007/978-94-007-0211-0
[15] Anderson H H 1960 Solvent extraction process for plutonium
[16] Bardez I 2004 *Etude des caractéristiques structurales et des propriétés de verres riches en terres rares destinés au confinement des produits de fission et éléments à vie longue* Ph.D. thesis Université Pierre et Marie Curie
[17] Taylor R J, Gregson C R, Carrott M J, Mason C and Sarsfield M J 2013 *Solvent Extraction and Ion Exchange* **31** 442–462 DOI: 10.1080/07366299.2013.800438
[18] Alonso J I G, Sena F, Arbore P, Betti M and Koch L 1995 *J. Anal. At. Spectrom.* **10** 381–393 DOI: 10.1039/JA9951000381
[19] Manheimer W M, Lampe M and Joyce G 1997 *J. Comput. Phys.* **138** 563–584 DOI: 10.1006/jcph.1997.5834

The Princeton Plasma Physics Laboratory is operated
by Princeton University under contract
with the U.S. Department of Energy.

Information Services
Princeton Plasma Physics Laboratory
P.O. Box 451
Princeton, NJ 08543

Phone: 609-243-2245
Fax: 609-243-2751
e-mail: pppl_info@pppl.gov
Internet Address: http://www.pppl.gov